Spectral bandwidth of interictal fast epileptic activity characterizes the seizure onset zone

Marcel Heers[a,b,c,*], Moritz Helias[d], Tanguy Hedrich[e], Matthias Dümpelmann[a,c], Andreas Schulze-Bonhage[a,c], Tonio Ball[a,b,c]

[a] Epilepsy Center, Department of Neurosurgery, Medical Center — University of Freiburg, Faculty of Medicine, University of Freiburg, Germany
[b] Translational Neurotechnology Lab, Department of Neurosurgery, Medical Center — University of Freiburg, Faculty of Medicine, University of Freiburg, Germany
[c] Cluster of Excellence BrainLinks-BrainTools, University of Freiburg, Germany
[d] Institute of Neuroscience and Medicine (INM-6) and Institute for Advanced Simulations (IAS-6), Jülich Research Centre and JARA, Jülich, Germany
[e] Multimodal Functional Imaging Lab, Biomedical Engineering Department, McGill University, Montreal, Québec, Canada

ARTICLE INFO

ABSTRACT

The foremost aim of presurgical epilepsy evaluation is the delineation of the seizure onset zone (SOZ). There is increasing evidence that fast epileptic activity (FEA, 14–250 Hz) occurring interictally, i.e. between seizures, is predominantly localized within the SOZ. Currently it is unknown, which frequency band of FEA performs best in identifying the SOZ, although prior studies suggest highest concordance of spectral changes with the SOZ for high frequency changes. We suspected that FEA reflects dampened oscillations in local cortical excitatory-inhibitory neural networks, and that interictal FEA in the SOZ is a consequence of reduced oscillatory damping. We therefore predict a narrowing of the spectral bandwidth alongside increased amplitudes of spectral peaks during interictal FEA events. To test this hypothesis, we evaluated spectral changes during interictal FEA in invasive EEG (iEEG) recordings of 13 patients with focal epilepsy. In relative spectra of beta and gamma band changes (14–250 Hz) during FEA, we found that spectral peaks within the SOZ indeed were significantly more narrow-banded and their power changes were significantly higher than outside the SOZ. In contrast, the peak frequency did not differ within and outside the SOZ. Our results show that bandwidth and power changes of spectral modulations during FEA both help localizing the SOZ. We propose the spectral bandwidth as new source of information for the evaluation of EEG data.

1. Introduction

Epilepsy is one of the most common neurological disorders that affects 70 million people worldwide (Ngugi et al., 2010). It consists of recurrent seizures that presumably occur as a result of disturbed synaptic excitation and inhibition (Jiruska et al., 2013). Approximately 60% of all epilepsy patients suffer from focal epilepsy (Zarrelli et al., 1999) and drug resistant focal epilepsy accounts for 30% of all focal epilepsies (Schuele and Lüders, 2008). In these patients it is hence one of the main aims to localize and characterize the SOZ. In some but not all patients the SOZ spatially correlates closely with structural cerebral abnormalities or with epileptic activity in between epileptic seizures, i.e. interictal activity (Rosenow and Lüders, 2001). Pathological changes related to epilepsy that are interictally observed in electrophysiological recordings are usually more extended than the SOZ. Apart from epileptic spikes these changes include fast oscillatory patterns in the β, γ and high γ band > 14 Hz (fast epileptic activity (FEA); de

Curtis et al., 2012). Recently, there is an increased interest in interictal FEA as it may help in the definition of the SOZ for the planning of epilepsy surgery (Bartolomei et al., 2008; Engel et al., 2009; Ren et al., 2015).

Previous studies have focused on a number of parameters characterizing interictal FEA, such as the number of events per time, their co-occurrence with epileptic spikes, and the frequency range of oscillations; for example the distinction of high frequency oscillations (HFOs) between ripple or fast ripple bands from 80 to 250 and 250 to 500 Hz, respectively (Zijlmans et al., 2012). However, a basic parameter of FEA has so far been neglected: its spectral bandwidth, i.e., the width of the peaks reflecting FEA in the spectral domain. Spectral bandwidth may be important as it closely relates to the damping of an oscillation, which describes how quickly an oscillation decays in amplitude. Spectral bandwidth may thus be informative with respect to epilepsy-related oscillations. Specifically, reduced bandwidth together with increased peak amplitude would indicate reduced damping of the

---

* Corresponding author at: Epilepsy Center, Department of Neurosurgery, University Medical Center Freiburg, Breisacher Str. 64, D-79106 Freiburg, Germany.
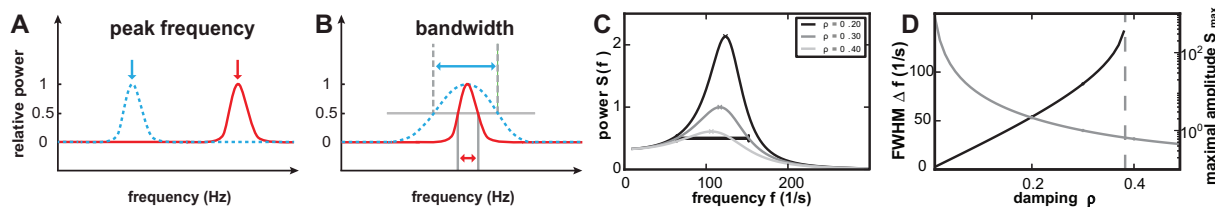*E-mail address:* marcel.heers@uniklinik-freiburg.de (M. Heers).

Fig. 1. Concept of spectral bandwidth changes. Generally, spectral changes may differ with respect to the peak frequency of the responses (A). However, even if responses have the same peak frequency, they may differ with respect to their spectral bandwidth (blue and red curves in B). Gray lines indicate the full width at half maximum (FWHM): the width at which the amplitude decays to half its maximum value. (C) Power spectrum of a harmonic oscillator for different values of the damping, normalized to the peak value for damping constant $\rho = 0.3$. The FWHM is indicated for the curve of $\rho = 0.3$. (D) Inverse Q factor (black) as a function of the damping constant ρ. Peak value of the power spectrum as a function of the damping (gray). The dashed vertical line indicates the limit for which a FWHM can be defined. Beyond this line, the power does not decay below half the peak value at small frequencies. (For interpretation of the references to color in this figure legend, the reader is referred to the web version of this article.)

underlying oscillation (Fig. 1). Reduced damping has been described in evoked cortical responses in generalized epilepsy (Lee et al., 1980). Also theoretical models describe seizure generation as a process during which cortical network dynamics approach a critical point which is a phase transition from interictal to seizure activity (Breakspear, 2005; Izhikevich, 2000; Jirsa et al., 2014). Interictal FEA in the SOZ may therefore be characterized by reduced damping, but a quantitative analysis of corresponding signatures in the spectral properties of FEA is so far lacking.

Intracranial EEG (iEEG) recordings during presurgical evaluation of epilepsy patients allow us to assess bandwidth and power changes associated with FEA events recorded directly from the cortical surface both in and outside of the SOZ. To quantify bandwidth changes in conjunction with other spectral parameters, we analyzed FEA-related relative spectral power modulations and mapped those relative to the SOZ. We show that bandwidth and spectral power changes differ between SOZ and non-SOZ contacts, whereas the peak frequency is not informative about the SOZ. Thus, FEA in the SOZ carries the predicted spectral signatures of reduced oscillatory damping. We argue that damping-related spectral changes not only shed new light on epilepsy-related oscillations, but may be relevant for pathological oscillatory activity in a broad range of neurological and possibly also psychiatric diseases that involve a cortical disbalance of synaptic excitation and inhibition.

2. Patients and methods

2.1. Patient selection

All 13 patients included in the analysis underwent elaborated clinical iEEG evaluation for drug resistant focal epilepsy at the University

Epilepsy Center Freiburg between 2006 and 2009. Initially we screened data of 22 epilepsy patients with at least one 64-contacts electrode grid implanted for presurgical epilepsy evaluation. These extended cortical recordings with high spatial resolution allow us to map the spatial distribution of spectral changes accurately. A secondary aim of our study is to develop parameters that can be used in future studies to objectify the clinical performance, e.g., of novel grid electrodes of the same size with high contact density.

The ethics committee of the University Medical Center Freiburg approved this study and all patients gave their written informed consent to the scientific use of their clinical data recorded during their presurgical evaluation at the University Epilepsy Freiburg. Eight of 22 patients were excluded, because no FEA was detected on the 64-contacts grid electrode. One of 22 patients was excluded, because no habitual seizures occurred during iEEG acquisition and thus the SOZ could not be defined.

For each of the 13 patients included, we compared the bandwidth analysis to clinical findings from their presurgical evaluation. For the comparison of spectral changes, we defined SOZ positive contacts concordant to the clinical reports. When different seizure types were reported, all contacts involved at seizure onset were counted as SOZ-positive contacts. Surgical resection of the epileptic focus was performed in 12/13 patients included in our study. Histological analysis of the resected specimens in those 12 patients who underwent surgical resection revealed focal cortical dysplasia (FCD) type I in 5/12 patients and FCD type II in 6/12 patients according to the classification of FCDs (Palmini et al., 2004). In 1/12 patient no histological assignment of the resected specimen was possible (Table 1).

The average follow-up for postsurgical outcome was 3.8 years (range 1–8 years). The postsurgical outcome was Engel 1 in six, Engel 2 in two, Engel 3 in three, and Engel 4 in 1 patient (Table 1) (Engel et al.,

Table 1
Clinical characteristics of included patients.

ID	Age	Seizure types	Location of implanted electrodes	SOZ	Histological specimens	No trials FEA	Hours of raw data	Postsurgical outcome
1	17	FS, FDS	G: RFP	RF	FCD 1B	709	2	1a (2)
2	23	FDS, sGTCS	G: RFP; RiH, RFL, RFB strips	RF	FCD 2A	862	6	1a (3)
3	51	FS, FDS, sGTCS	G: LF; LFL, LFP, LiH strips	LF	FCD 1B	174	4	2b (1)
4	40	FDS, sGTCS	G: LF; LFP, LiH strips	LF	FCD 2A	286	4	1a (5)
5	38	FS, FDS, sGTCS	G: LFP; LFB, LFL, LiH strips	LF	FCD 1A	1060	1	3a (4)
6	14	FDS, sGTCS	G: LTPO; LTB, LOPM, LOPL strips	LOP	FCD 2A	1339	1	4a (2)
7	27	FS	G: LFP; LiH strips, 2 DE: LIn	LF	FCD 1B	373	5	1a (5)
8	57	FDS, sGTCS	G: LFTPO; FP, TB, TL, POL, OM strips, DE: LH	LO	N/A	2512	1	3a (8)
9	34	FS, FDS, sGTCS	G: RFTP; RiH strips	RP	N/A	2242	1	N/A
10	58	FS, FDS, sGTCS	G: RTPO, RTL, RTB strips, DE: RH	RO	FCD 1A	149	6	1c (4)
11	42	FS, FDS, sGTCS	G: RFP	RF	FCD 2B	1077	1	1a (1)
12	21	FS	G: LF	LF	FCD 2A	1181	5	2a (5)
13	17	FS, FDS, sGTCS	G: RFP; RFB, RFL, RiH strips	RF	FCD 2A	553	3	3a (5)

Patient data and clinical findings, implanted electrodes, histological findings, hours of raw data visually evaluated for FEA (fast epileptic activity) and baselines, postsurgical outcomes according to the Engel classification and follow up time (in years): DE: depth electrode, FB: fronto-basal, FCD: focal cortical dysplasia, FP: frontopolar, FDS: focal dyscognitive seizures, FL: fronto-lateral, FS: focal seizures, G: 8 × 8 contacts quadratic subdural grid electrode, H: hippocampus, iH: inter-hemispheric, In: insula, L: left, R: right, M: mesial, N/A: not available, O: occipital lobe, P: parietal lobe; sGTCS: secondarily generalized tonic-clonic seizures, T: temporal lobe.

1993). Thus the postsurgical outcome in our group of patients is worse compared to typical patients with structural epilepsy (70–80% seizure free outcome) (Fauser et al., 2004; Wagner et al., 2011). In this cohort, both the need to use extended iEEG and the need to spare eloquent brain areas in close proximity to the epileptogenic zone contribute to a bias to difficult-to-treat epilepsies.

2.2. IEEG analysis

2.2.1. IEEG acquisition and identification of FEA

IEEG can be acquired using subdural grid and depth electrodes. In our study, in all patients at least one subdural grid electrode with 8 × 8 contacts was implanted (contact diameter: 4 mm, exposed contact surface diameter: 2.3 mm, center-to-center inter-contact distance: 10 mm; AD-tech, Racine, WI, USA). In some patients additional strip electrodes with the same inter-contact distance were used. In three patients (ID 7, 8, 10) additional depth electrodes with 10 contacts each (electrode diameter: 0.8 mm, contact length: 2 mm, inter-contact distance: 1.5 mm, Dixi-Medical, Besancon, France) were implanted. IEEG was acquired from a total number of 1147 contacts (mean per patient: 88, range: 63–120) in the entire group of patients. The iEEG was recorded at a sampling rate of 1024 Hz, using a Neurofile NT digital video-EEG system with 128 channels and a 16-bit A/D converter. The built-in high-pass filter had a time constant of 1 s (cut-off frequency ~ 0.16 Hz) and a low-pass filter with a cut-off frequency of 344 Hz.

We analyzed the iEEG data for FEA events using the following criteria. We visually marked onset and end of FEA events (length 0.5–10 s) for each patient in the first night showing good data quality (Fig. 2). Whenever available the first night with simultaneous iEEG/scalp EEG data was chosen instead to facilitate sleep staging. The interictal FEA patterns were selected as illustrated in figures of prior studies: Fig. 1, patterns C and D (Fauser and Schulze-Bonhage, 2006) and Fig. 1, patterns 2 and 3 (Menezes Cordeiro et al., 2015). We evaluated a time window of 1–6 h of non-rapid eye movement (NREM) sleep between 11 pm and 6 am. We chose to mark events between 11 pm and 6 am to reduce the brainstate-dependent changes of FEA and to benefit from the more frequent occurrence of FEA during sleep (Boonyapisit et al., 2003; Tassi et al., 2012). Sleep staging was done based on simultaneous surface EEG recordings in 6/13 patients and less reliably based on iEEG and video data in 7/13 patients. The amplitude of the marked events was considerably different in the β-γ frequency band compared to baseline. The analyses were performed by a certified epileptologist (M.H.) according to the clinical EEG reviewing standards of the American Society of Clinical Neurophysiology (http://www.acns.org/practice/guidelines) using the clinical data browser of IT-med software (Natus Europe, Planegg, Germany). The time resolution was 5–10 s per 21-in. 4:3 computer screen. 32–50 iEEG traces were displayed at a time without overlap. Built-in high-pass-filter with a time-constant of 0.3 (0.531 Hz) and no further low-pass filtering was applied. A 50-Hz notch filter was added whenever required. The onset and end of β and γ FEA patterns were marked in bipolar and verified in common average reference montages. FEA patterns were usually distributed across multiple contacts and the marking was done in one contact with the most prominent FEA activity per patient. Only one FEA pattern type was marked per patient. Automatic detectors validated for our tasks were not available for this study and will be tested and validated as part of future projects. During visual inspection of the FEA the reviewer was blind to findings from presurgical evaluation, e.g. the distribution of the seizure onset zone and the postsurgical outcome. The distance in time of the marked segments before and after the previous/next clinical seizure was at least 1 h.

Baselines were selected from NREM sleep segments in a matched number and duration of trials per patient in between FEA trials. We aimed to select baselines from deep sleep stage (mainly stages II–III, because patients seldom reached sleep stage IV during intracranial implantations). Results were tested for their reproducibility using varying baseline segments, e.g. using baselines from sleep stage II only.

2.2.2. IEEG pre-processing and spectral analysis

IEEG data were re-referenced and cut into trials for transformation in the frequency domain. We re-referenced the iEEG data of each contact against the mean of all regional iEEG, e.g. all other frontal contacts or all interhemispheric contacts. This regional averaged reference has the advantage that it does not artificially spread signal changes towards distant brain regions. In patients with simultaneous subdural and depth electrodes, references were calculated for each electrode type separately. FEA and baseline segments were cut into 0.5-s trials with 50% overlap. The same number of baseline trials as FEA trials was chosen for each patient. For spectral analysis, FEA trials and baseline trials were multiplied with a Blackman window function of 512 sampling points length covering the whole 0.5-s trial and transformed to the frequency domain using the fast Fourier transformation as implemented in Matlab 2014b (MathWorks, Natick, MA, United States; all further analysis steps were also implemented in Matlab 2014b). Our parameters resulted in a nominal frequency resolution of 2 Hz. For the signals from each iEEG contact we divided the median power across FEA trials at each frequency by the corresponding values across the baseline trials in order to calculate the relative spectra.
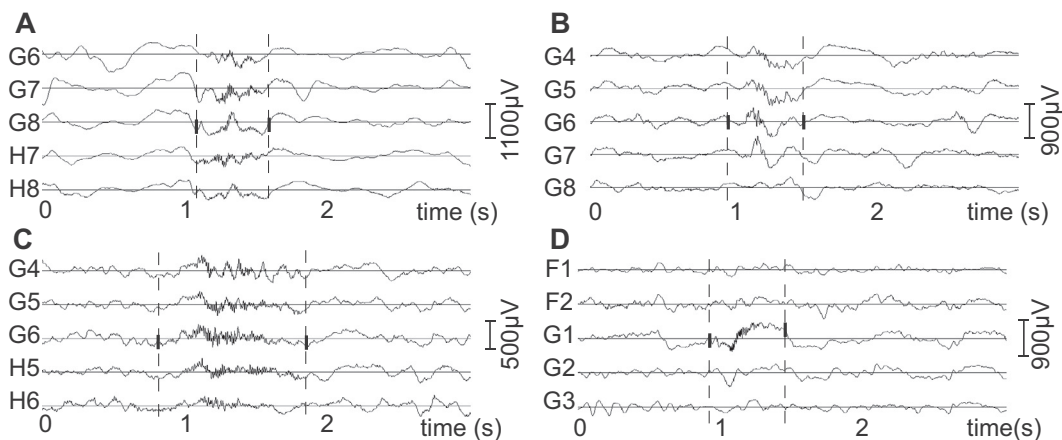

Fig. 2. Examples of fast epileptic activity (FEA) epochs for patients 5 (A), 6 (B), 7 (C), 9 (D) (common average reference) on selected invasive EEG grid contacts from the 64 contacts grid electrodes. Bold, vertical lines illustrate visually marked onset and end of FEA epochs in traces in which this event type was marked. Dashed, vertical lines extend these markers to traces of neighboring contacts.
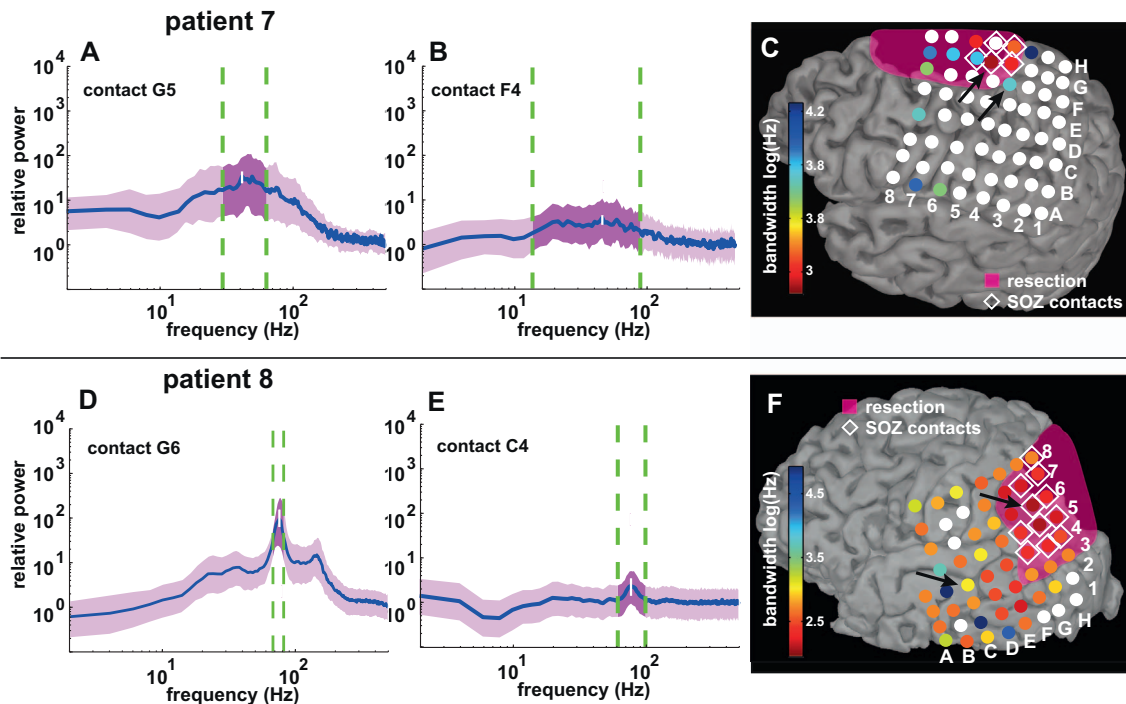
Fig. 3. iEEG γ peaks (A, B, D, E) and spectral bandwidth distributions (C and F) and in two example patients (patients 7 and 8): panels A, B (patient 7: contacts G5 and F4) D, E (patient 8: contacts G6 and C4) illustrate relative spectra of four different grid contacts. For each panel the blue line denotes the median signal and the purple trace shows the spectral changes between the 25th and 75th percentile of the signal variance. The vertical white line marks the frequency with highest power (maximum power). The vertical dashed green lines enclose the spectral width at full width half max (FWHM) of the spectral peak. A and D illustrate relatively narrow-banded spectral peaks within the SOZ, whereas B and E are relatively broad-banded and outside the SOZ (black arrows panels C and F). Please note that the spectral peak in panel D can be subdivided visually into two distinct maxima. This finding could be reproduced in single trial time-frequency analysis (Fig. Suppl. 1).

C and F show bandwidth changes illustrated on invasive EEG grid contacts co-registered with segmentations of individual cortical surfaces reconstructed from MRIs after surgical resection of the epileptic focus for both patients. Each disk represents one electrode contact. Seizure onset zone (SOZ) contacts are marked with white diamonds. The coloring of the grid contacts denotes bandwidth in log (Hz). White disks represent electrode contacts that were not considered in the comparison, because either no spectral peaks with peak frequencies > 40 Hz could be detected or no significant spectral changes compared to baseline were recorded in the frequency band of the median spectral peak. The resection volume is marked in transparent magenta. The two patients represent two extremes in the range of bandwidth changes: patient 7 exhibits broad-banded spectral maxima in a limited number of contacts, whereas spectral peaks in patient 8 are spatially more distributed and relatively narrow-banded. (panels C and F were created using brainVISA and brainstorm software Mangin et al., 1995; Tadel et al., 2011). (For interpretation of the references to color in this figure legend, the reader is referred to the web version of this article.)

2.2.3. Statistical analysis

FEA-related spectral changes were significance-tested against baseline at a level of $q < 0.0001$ using Wilcoxon Ranksum test and false discovery rate (FDR) correction (Benjamini and Hochberg, 1995). Only iEEG contacts for which spectral changes fulfilled these statistical criteria were considered for subsequent detection of spectral peaks. When only γ-changes were considered, one patient (ID 2) was excluded, because no spectral peaks outside the SOZ were detected for this patient in this frequency band.

2.2.4. Parameters of spectral changes

For each iEEG contact, the median of the relative spectrum at each contact was calculated and the local maximum within the frequency range of either 40–250 Hz (γ peaks) or 14–250 Hz (β-γ peaks) was identified as the peak frequency. The power value at this frequency was defined as maximum power. The FWHM corresponding to this peak, i.e. the range in frequency where the signal is higher than half of the maximum power, was computed. The Q factor was defined as the ratio between the peak frequency and the bandwidth (the length of the FWHM) for each spectral peak.

To study correlations between bandwidth parameters and the number of FEA events per time we computed the Kendall Rank Correlation Coefficient between the FEA counts per hour and the mean peak frequency, bandwidth, Q factor, and maximum power per patient (Kendall, 1970). For this comparison we included all identified spectral peaks per patient (inside and outside the SOZ) and compared all four parameters to the FEA counts for the β-γ and γ band separately.

2.2.5. Comparison of SOZ and non-SOZ contacts

It was our aim to analyze the relation of bandwidth changes of the spectral peaks to SOZ positive contacts to estimate the relevance of these spectral changes for characterizing the SOZ. To this end we first computed the median-values of all parameters of interest (peak frequency, bandwidth, Q factor and maximum power of the identified spectral peaks) for SOZ-positive and SOZ-negative contacts per patient. This resulted in four pairs of median values for each parameter that were evaluated in β and γ band in each patient. Median values were to increase the robustness against single outliers. For pairwise statistical comparison of these median values for SOZ-negative and SOZ-positive contacts per patient we used the sign test (Koti and Babu, 1996).

2.2.6. Individual patients analysis

For the comparison of the overlap between the spectral parameters and the SOZ in individual patients we used area under the receiver operating characteristics curve (AUC) comparisons (Heers et al., 2014; Metz, 1986). The method compares sensitivities and specificities of a diagnostic parameter for different thresholds summarized in a single value. AUC values allow comparing overlap of a diagnostic marker with the ground truth, which are in our study the iEEG contacts within the SOZ. As AUC values > 0.7 are usually considered as good overlap between diagnostic marker and ground truth, we chose this threshold to identify patients in whom we had good overlap between iEEG contacts within the SOZ and the spectral parameters peak frequency, bandwidth, Q factor, and maximum power.

2.2.7. Single trial time-frequency analysis

To further confirm our finding from averaged spectra over multiple trials, we performed single-trial time-frequency analysis for contacts with visually distinguishable multiple spectral maxima. Time-frequency analysis was added as a qualitative method to also consider the evolution of the FEA events over time, but no further quantification of the results was carried out. Time-intervals from 2 s before to 4 s after the onset of marked FEA intervals were analyzed. The time window from − 2 to − 1 s was considered as averaged baseline over all analyzed trials per patient. EEG data were transformed to the time-frequency domain using a sliding window of 0.5 s length and a feed forward rate of 62.5 ms. For the computation of the trial-averaged spectra we used a single taper spectral decomposition as described above, to keep the frequency resolution high. For the single-trial analysis we chose a multitaper spectral analysis with five Slepian tapers, treating frequency resolution against signal-to-noise, which was useful for single-trial evaluation of the spectra.

3. Results

Spectral peaks were identified in a variable number of iEEG contacts within the group of patients. Spectral peaks were defined as power maxima per contact with available lower and higher FWHM (full width half maximum) values between 14 Hz and 250 Hz with significant spectral changes during FEA compared to baseline ($q < 0.0001$, Wilcoxon Ranksum Test, FDR correction). For the γ band analysis, significant spectral peaks were detected in a total number of 413/1147 contacts (32 contacts per patient on average, range: 1–75). Bandwidth at FWHM, and maximum power of the detected spectral γ peaks varied within patients (maximum power; Fig. 1, Fig. 3). Peak frequency (mean 111, STD 108 Hz), spectral bandwidth (mean: 34 Hz, STD: 27 Hz), the frequency-normalized bandwidth named Q factor (mean: 0.51, STD: 0.42) and maximum power (mean: 25, STD: 56) varied considerably across patients (Table 2, Fig. 3). Results were similar for the combined analysis of spectral peaks in β-γ frequency bands with peak frequencies > 14 Hz. Significant spectral peaks during FEA were detected in a total number of 446/1147 contacts (34 contacts per patient, range: 6–87). Spectral peaks again varied considerably in their peak frequency (mean 70, STD: 87 Hz), spectral bandwidth (mean: 33 Hz, STD: 28 Hz), Q factor (mean: 0.69 STD: 0.99) and maximum power (mean: 29, STD: 75) within the group of patients (Table 2).

Spectral bandwidth, Q factor and maximum power, but not the maximal frequency of spectral peaks differed significantly between SOZ and non-SOZ contacts (Fig. 4). Comparing median bandwidths of spectral changes per patient with SOZ contacts we found that bandwidth changes were more narrow-banded in SOZ contacts than bandwidth changes in non-SOZ contacts (γ: $p = 0.039$; β-γ: $p = 0.003$, sign test). Similar to bandwidth changes the Q factor was lower (γ: $p = 0.039$; β-γ: $p = 0.00024$, sign test) and maximum power (γ: $p = 0.00024$; β-γ: $p = 0.0002$, sign test) was higher for SOZ contacts than for non-SOZ contacts in all patients. In contrast to bandwidth and maximum power changes, the peak frequency of spectral peaks was similar between SOZ and non-SOZ contacts (γ: $p = 0.34$; β-γ: $p = 1$, sign test) (Fig. 3). Thus, spectral bandwidth and power changes differed significantly between SOZ and non-SOZ contacts, but not their peak frequency.

Despite this generally clear relation of bandwidth changes and the SOZ, findings varied inter-individually between two scenarios. In some patients, relatively broad-banded spectral peaks occurred in a low number of contacts (example: Fig. 2, patient 7). In other patients more narrow-banded spectral peaks were detected in a larger number of contacts (example: Fig. 2, patient 8). Especially in this second group of patients we observed multiple, simultaneously occurring power maxima most often within the group of SOZ contacts (Fig. 2, patient 8). Power maxima in distinct frequency bands often co-occurred simultaneously. Seldom, spectral changes evolved over time (Fig. Suppl. 1). All resected specimens with histological assignment were classified as focal cortical dysplasia (FCD; Table 2); we did not find any correlation of specific bandwidth changes, peak frequencies or maximum power changes with specific FCD subtypes or lobar localization of pathological changes. The comparison between the number of identified events per hour and mean peak frequency, bandwidth, Q factor, and maximum power only showed significant correlations between the peak frequency and the number of events for the γ band ($p = 0.02$, rτ = 0.45, Kendall Rank Correlation Coefficient). All other parameters were not significantly correlated with FEA counts, neither for the β-γ, nor for the γ band.

At the individual patient level we found good overlap between bandwidth, Q factor, and maximum power with the SOZ in the majority of patients as shown by AUC values > 0.7 (Table 3). Similar to the group comparison peak frequencies differed seldom within and outside the SOZ resulting in AUC values > 0.7 in only a minority of patients (β-γ-band: 2/13 patients, γ-band: 4/12 patients). In contrast, bandwidth and Q factor showed good detection of the SOZ with AUC values > 0.7 (β-γ: bandwidth: 10/13 patients, Q factor: 8/13; γ: 8/12 patients Q factor: 6/12). Maximum power performed best in this comparison with

Table 2
Results of spectral evaluation.

ID	No. C SOZ	γ frequency band					β-γ frequency band				
		No. C spectral peaks	Peak frequency (Hz)	Bandwidth (Hz)	Q factor	Maximum power	No. C spectral peaks	Peak frequency (Hz)	Bandwidth (Hz)	Q factor	Maximum power
1	16	23	64 ± 10	29 ± 33	0.45 ± 0.44	7 ± 8	22	64 ± 10	29 ± 34	0.44 ± 0.45	7 ± 8
2	3	1	58 ± 0	29 ± 0	0.50 ± 0.00	8 ± 0	13	24 ± 4	15 ± 6	0.62 ± 0.28	8 ± 5
3	8	65	44 ± 13	19 ± 4	0.44 ± 0.09	95 ± 107	85	32 ± 6	14 ± 3	0.46 ± 0.14	109 ± 141
4	8	13	62 ± 24	64 ± 55	1.07 ± 0.82	5 ± 5	22	39 ± 27	42 ± 46	1.03 ± 0.66	6 ± 8
5	6	69	94 ± 12	37 ± 15	0.40 ± 0.16	13 ± 14	55	93 ± 11	36 ± 16	0.38 ± 0.17	14 ± 15
6	15	51	105 ± 11	46 ± 20	0.44 ± 0.19	8 ± 8	51	105 ± 11	46 ± 20	0.44 ± 0.19	8 ± 8
7	5	18	49 ± 8	38 ± 13	0.80 ± 0.30	7 ± 9	23	38 ± 15	39 ± 18	1.27 ± 1.00	7 ± 8
8	19	63	77 ± 3	20 ± 24	0.25 ± 0.30	12 ± 22	63	77 ± 3	20 ± 24	0.25 ± 0.30	12 ± 22
9	13	8	102 ± 5	40 ± 21	0.40 ± 0.22	5 ± 2	8	102 ± 5	40 ± 21	0.40 ± 0.22	5 ± 2
10	3	15	93 ± 26	25 ± 12	0.30 ± 0.20	4 ± 3	15	93 ± 26	25 ± 12	0.30 ± 0.20	4 ± 3
11	10	10	70 ± 13	77 ± 37	1.15 ± 0.71	3 ± 1	22	39 ± 26	70 ± 52	2.66 ± 2.90	2 ± 1
12	9	35	48 ± 10	54 ± 37	1.10 ± 0.54	7 ± 6	40	40 ± 11	52 ± 27	1.48 ± 1.09	6 ± 6
13	23	23	74 ± 16	25 ± 11	0.34 ± 0.15	31 ± 42	14	74 ± 13	24 ± 12	0.33 ± 0.17	46 ± 48

Number of SOZ channels, spectral peaks with significant spectral changes during fast epileptic activity (FEA) compared to baseline (q level < 0.001, Wilcoxon Ranksum Test, FDR correction) and mean values ± standard deviations of peak frequency, bandwidth, Q factor and maximum power, for individual patients, C: contacts. Please note the wide range of bandwidth and power within and between patients.
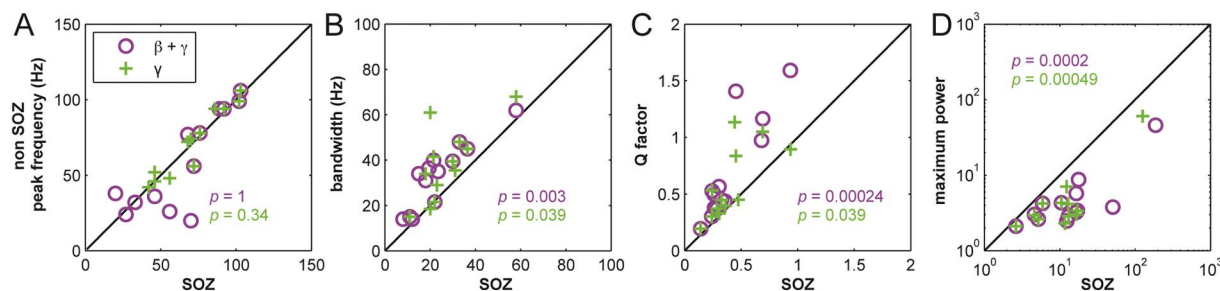
Fig. 4. Comparison of median relative peak frequency (A), bandwidth (B), Q factor (C) and maximum power (D) for contacts inside the seizure onset zone (SOZ contacts) and for contacts outside the seizure onset zone (non-SOZ) per patient for β-γ peaks (peak frequency > 14 Hz ($N = 13$ patients); γ peaks: peak frequency > 40 Hz ($N = 12$ patients). Changes of bandwidth, Q factor and maximum power differ significantly between SOZ and non-SOZ contacts for both frequency bands, whereas the peak frequency is similar between SOZ and non-SOZ contacts, but widely differs between patients. Magenta circles: median values for spectral β-γ peaks; green cross: median values for spectral γ peaks. This latter comparison was impossible for patient 9, because no spectral peaks were detected in contacts outside the SOZ. *p*-values report results of the sign test. (For interpretation of the references to color in this figure legend, the reader is referred to the web version of this article.)

AUC values > 0.7 in 13/13 patients (β-γ) and 12/12 patients (γ).

4. Discussion

Our results show that bandwidth, Q factor and amplitudes of FEA-related spectral changes all inform about cortical disfunction in focal epilepsy, regardless the peak frequency of these changes. The observed narrow-banded spectral peaks in a wide range of peak frequencies during FEA as a characteristic of the SOZ in patients with focal epilepsy thus introduces a new concept for iEEG interpretation, that is decisive beyond the peak frequency (Staba et al., 2007).

In neocortical epilepsy, FEA is typically associated with FCDs (Nobili et al., 2009; Palmini et al., 2004; Tassi et al., 2012). Our findings underline these observations, since all included patients with assigned pathology suffered from focal epilepsy related to FCDs. Despite similar histological findings, spectral bandwidths and peak frequencies differed widely in our group of patients. Interestingly, the number of identified spectral peaks and their spectral profile in the individual patient was unrelated to specific histological subtypes.

In the majority of the individual patients spectral bandwidth parameters and maximum power recovered the spatial extent of the SOZ using the AUC method. In contrast there was no clear association between the peak frequency and the SOZ using the AUC method. The performance of the parameters described in this study may be enhanced by studying their mixed effect using machine learning algorithms (Dümpelmann et al., 2015) to further improve the overlap with the SOZ. Additionally, microelectrodes for iEEG with a higher density of

smaller contacts (Henle et al., 2011) compared to standard iEEG electrodes may allow to better disentangle two major causes of increased bandwidth. Bandwidth may be either increased due to network damping within one localized cortical population, as suggested as a mechanism here. Alternatively, bandwidth may be increased due to averaging over multiple neural populations with more narrow-banded spectral signatures (Crone et al., 2011). These new iEEG electrodes may enable a more accurate delineation of the SOZ based on spectral bandwidth changes as it has been shown for micro seizures before (Stead et al., 2010).

From a theoretical point of view the observed relationship between the width of the spectral peak and its maximal amplitude is a common feature shared by many systems exhibiting oscillatory behavior. Theoretical work has shown that fast oscillations in recurrent neuronal networks in the γ band result from dominant negative and delayed feedback (Brunel, 2000). Such feedback is required for stability of balanced networks (van Vreeswijk and Sompolinsky, 1996). Even below the point where the system produces self-sustained and ongoing oscillations, power spectra of the fluctuating dynamics in such networks show a pronounced peak close to a dominant oscillation frequency, typically in the γ or high γ regime (Helias et al., 2013). The prototype of such a resonant system is the classical harmonic oscillator. We use this model in Fig. 1 (panels C and D) to illustrate the fundamental relationship between the damping of the oscillation (controlling how quickly an oscillation decays in amplitude), the peak value observed in the power spectrum, and the width of the peak (see appendix Q factor for details). With increasing damping, the peak amplitude decreases

Table 3
Spectral markers and SOZ in individual patients.

γ frequency band					β-γ frequency band			
AUC					AUC			
ID	Peak frequency	Bandwidth	Q factor	Maximum power	Peak frequency	Bandwidth	Q factor	Maximum power
1	0.70	0.90	0.95	0.82	0.67	0.88	0.94	0.80
2	N/A	N/A	N/A	N/A	0.73	0.98	1	1
3	0.62	0.35	0.40	0.76	0.56	0.6	0.65	0.79
4	0.35	0.97	0.92	0.94	0.21	0.93	0.75	1
5	0.28	0.63	0.52	0.70	0.30	0.71	0.62	0.72
6	0.48	0.73	0.72	0.93	0.47	0.72	0.72	0.93
7	0.70	0.83	0.93	0.93	0.86	0.80	0.95	0.93
8	0.35	0.84	0.83	0.92	0.35	0.84	0.83	0.92
9	0.63	0.75	0.69	0.81	0.63	0.75	0.69	0.81
10	0.49	0.47	0.58	0.94	0.49	0.47	0.58	0.94
11	0.5	0.76	0.64	0.72	0.9	0.53	0.65	0.75
12	0.60	0.79	0.76	0.90	0.80	0.82	0.86	0.91
13	0.4	0.59	0.57	0.83	0.46	0.83	0.83	1

Comparison between contacts within and outside the seizure onset zone (SOZ) using area under the receiver operating characteristics curve (AUC) between iEEG contacts of individual patients, N/A. In patient 2 in the γ frequency band no spectral peaks were detected outside the SOZ, so no AUC comparison was possible.

and at the same time the bandwidth, measured as FWHM, increases. The location of the peak frequency, however, is only marginally influenced by the damping, slightly decreasing with higher damping. The less the damping, the closer the system is to the critical point at which ongoing oscillations of high amplitude set in. In neuronal networks, the effective damping, or equivalently, the closeness to the critical point, is controlled by a variety of network parameters (Helias et al., 2014). Parameters that are most effective in changing the oscillatory properties are the external excitatory input that a local cortical network receives, increasing the tendency to oscillate with increasing drive and the balance between excitatory and inhibitory recurrent connections within the local network, where an increase of the effective inhibitory feedback within the network promotes oscillations.

There is increasing evidence from ictal recordings that FEA is indeed associated with a disbalance between excitatory and inhibitory activity in FCD-related neocortical epilepsy (de Curtis and Gnatkovsky, 2009). Paradoxically, studies in animal models (Gnatkovsky et al., 2008) and on human FCD tissue (D'Antuono et al., 2004) report that excessive inhibition mediated by GABA-A-receptors can result in excessive excitation, eventually caused by failure of the inhibitory system. Simulations also support the concept of GABA-mediated disturbance of inhibition leading to FEA (Wendling et al., 2002). It however remains to be further explored how findings from ictal and interictal types of FEA relate to each other; the morphology of ictal and interictal FEA at least suggest a high degree of similarity.

Histopathological analyses of FCD tissue may lead to the point of view that FCDs are possible model lesions of disbalanced cortical excitation and inhibition (Spreafico et al., 1998). As all patients in our study with FEA and assigned pathology had FCDs, this specific kind of cortical pathology is closely associated with oscillatory discharges. Although no common pattern of histological changes could be established yet, pathological changes often involved lower layers of cortical tissue. FCDs consist of blurring of the cortical and subcortical junction. Ectopic subcortical neurons are surrounded by hypertrophic parvalbumin binding cells, the latter being basket and chandelier cells in layers IV and V of the cortical surface (Alonso-Nanclares et al., 2005; Nakagawa et al., 2017). It remains unclear, if parvalbumin binding cells are mainly dispersed over multiple layers (Medici et al., 2016) or if also the total number of parvalbumin cells is diminished in FCDs (Nakagawa et al., 2017). It is assumed that epileptic seizures arise from the dysplastic lesion itself (Chassoux et al., 2000). It thus remains worthwhile to continue studying alterations in the balance of cortical excitation and inhibition in FCDs to further unravel their epileptogenesis.

In the γ band we observe a correlation between the frequency of FEA events and the peak frequency of oscillations. A possible explanation for such a systematic dependence is that both phenomena are bifurcations of the network activity. In network models, gamma oscillations are caused by a Hopf bifurcation (Brunel, 2000; Brunel and Hakim, 1999). The frequency of the oscillation systematically depends, among other parameters, on the strength of the overall negative feedback (see parameter 'L' in Fig. 4b left panel in Helias et al., 2013). But the same parameter also controls the closeness to the saddle node bifurcation that marks the onset of the high activity state *synchronous regular* (SR) (see parameter 'g', Fig. 1B and Fig. 2 in Brunel, 2000). If FEA events can be associated with the latter bifurcation, possibly on a spatially more local scale fostered by local feedback, the correlation of the two measures seems to hint at the distance to the balanced point ($g = 4$ in Brunel, 2000) to be a common underlying control parameter, but future work is needed to investigate this hypothesis in more detail.

As an additional perspective for further research it is noteworthy that bandwidth differences, as we have demonstrated across cortical space, comparing SOZ with non-SOZ cortex, may as well exist across time. Specifically, the line of arguments that a narrowing of bandwidth signifies the approach of the cortical networks towards a critical point of seizure onset suggests that pre-ictal FEA spectra should narrow as the next seizure comes close. In the project on hand we did not compare

interictal to preictal FEA, as not enough seizures were recorded in the evaluated datasets and we could not show a significant correlation between the counts of FEA events and the spectral bandwidth. However, it will be intriguing to study FEA bandwidth changes for their potential in seizure prediction in future projects.

Besides seizure prediction, another area of intense clinical interest is the precise localization of the SOZ from interictal activity. During presurgical evaluation it is the aim to record seizures to determine the SOZ so that the epileptogenic zone (minimum cerebral area that needs to be resected to become seizure free) can be identified for epilepsy surgery (Rosenow and Lüders, 2001). Recording seizures during presurgical evaluation of epilepsy is demanding for patients and time-consuming. There is thus an increasing interest in interictal FEA in a broad frequency band between beta and gamma frequency bands (Aubert et al., 2009; Ren et al., 2015) and the ripples and fast ripple frequencies of HFOs (Jacobs et al., 2009; Worrell et al., 2004; Zijlmans et al., 2017). Our data prove that spectral bandwidth of FEA differs between contacts within and outside the SOZ for a broad range of frequencies that exceed ripple frequency band of HFOs [80–250 Hz] towards gamma and beta frequency bands > 14 Hz. Additionally, surgical removal of FEA may predict favorable post-surgical outcome (Aubert et al., 2009; Jacobs et al., 2010). Our present findings, that spectral signatures of reduced oscillatory damping of FEA characterize the SOZ, encourage similar studies on the postoperative predictive value of these novel markers, which was out of the scope of the current study. The clinical application of our new FEA markers may further be extended, if the here presented results transfer to scalp EEG and magnetoencephalography (MEG) data. This may well be the case as interictal FEA events as such have already been detected in EEG (Andrade-Valenca et al., 2011) and MEG recordings (von Ellenrieder et al., 2016).

Supplementary data to this article can be found online at https://doi.org/10.1016/j.nicl.2017.11.021.

References

Alonso-Nanclares, L., Garbelli, R., Sola, R.G., Pastor, J., Tassi, L., Spreafico, R., DeFelipe, J., 2005. Microanatomy of the dysplastic neocortex from epileptic patients. Brain 128, 158–173. http://dx.doi.org/10.1093/brain/awh331.
Andrade-Valenca, L.P., Dubeau, F., Mari, F., Zelmann, R., Gotman, J., 2011. Interictal

scalp fast oscillations as a marker of the seizure onset zone. Neurology 77, 524–531. http://dx.doi.org/10.1212/WNL.0b013e318228bee2.

Aubert, S., Wendling, F., Regis, J., McGonigal, A., Figarella-Branger, D., Peragut, J.-C., Girard, N., Chauvel, P., Bartolomei, F., 2009. Local and remote epileptogenicity in focal cortical dysplasias and neurodevelopmental tumours. Brain 132, 3072–3086. http://dx.doi.org/10.1093/brain/awp242.

Bartolomei, F., Chauvel, P., Wendling, F., 2008. Epileptogenicity of brain structures in human temporal lobe epilepsy: a quantified study from intracerebral EEG. Brain 131, 1818–1830. http://dx.doi.org/10.1093/brain/awn111.

Benjamini, Y., Hochberg, J., 1995. Controlling the false discovery rate: a practical and powerful approach to multiple testing. J. R. Stat. Soc. Ser. B 57, 289–300.

Boonyapisit, K., et al., Najm, I., Klem, G., Ying, Z., Burrier, C., LaPresto, E., Nair, D., Bingaman, W., Prayson, R., Lüders, H., 2003. Epileptogenicity of focal malformations due to abnormal cortical development: direct electrocorticographic-histopathologic correlations. Epilepsia 44, 69–76.

Breakspear, M., 2005. A unifying explanation of primary generalized seizures through nonlinear brain modeling and bifurcation analysis. Cereb. Cortex 16, 1296–1313. http://dx.doi.org/10.1093/cercor/bhj072.

Brunel, N., 2000. Dynamics of sparsely connected networks of excitatory and inhibitory spiking neurons. J. Comput. Neurosci. 8, 183–208.

Brunel, N., Hakim, V., 1999. Fast global oscillations in networks of integrate-and-fire neurons with low firing rates. Neural Comput. 11, 1621–1671.

Chassoux, F., Devaux, B., Landre, E., Turak, B., Nataf, F., Varlet, P., Chodkiewicz, J.P., Daumas-Duport, C., 2000. Stereoelectroencephalography in focal cortical dysplasia: a 3D approach to delineating the dysplastic cortex. Brain 123 (8), 1733–1751.

Crone, N.E., Korzeniewska, A., Franaszczuk, P.J., 2011. Cortical gamma responses: searching high and low. Int. J. Psychophysiol. http://dx.doi.org/10.1016/j.ijpsycho.2010.10.013.

D'Antuono, M., Louvel, J., Kohling, R., Mattia, D., Bernasconi, A., Olivier, A., Turak, B., Devaux, A., Pumain, R., Avoli, M., 2004. GABAA receptor-dependent synchronization leads to ictogenesis in the human dysplastic cortex. Brain 127, 1626–1640. http://dx.doi.org/10.1093/brain/awh181.

de Curtis, M., Gnatkovsky, V., 2009. Reevaluating the mechanisms of focal ictogenesis: the role of low-voltage fast activity. Epilepsia 50, 2514–2525. http://dx.doi.org/10.1111/j.1528-1167.2009.02249.x.

de Curtis, M., Jefferys, J.G.R., Avoli, M., 2012. Interictal epileptiform discharges in partial epilepsy: complex neurobiological mechanisms based on experimental and clinical evidence. In: Noebels, J.L., Avoli, M., Rogawski, M.A., Olsen, R.W., Delgado-Escueta, A.V. (Eds.), Jasper's Basic Mechanisms of the Epilepsies, (Bethesda, MD).

Dümpelmann, M., Jacobs, J., Schulze-Bonhage, A., 2015. Temporal and spatial characteristics of high frequency oscillations as a new biomarker in epilepsy. Epilepsia 56, 197–206. http://dx.doi.org/10.1111/epi.12844.

Engel, J.J., Van Ness, P., Rasmussen, T., Ojemann, L., 1993. Outcome with respect to epileptic seizures. In: Engel, J.J. (Ed.), Surgical Treatment of the Epilepsies. Raven Press, New York, pp. 615.

Engel, J., Jr., Bragin, A., Staba, R., Mody, I., 2009. High-frequency oscillations: what is normal and what is not? Epilepsia 50, 598–604.

Fauser, S., Schulze-Bonhage, A., 2006. Epileptogenicity of cortical dysplasia in temporal lobe dual pathology: an electrophysiological study with invasive recordings. Brain 129, 82–95. http://dx.doi.org/10.1093/brain/awh687.

Fauser, S., Schulze-Bonhage, A., Honegger, J., Carmona, H., Huppertz, H.J., Pantazis, G., Rona, S., Bast, T., Strobl, K., Steinhoff, B.J., Korinthenberg, R., Rating, D., Volk, B., Zentner, J., 2004. Focal cortical dysplasias: surgical outcome in 67 patients in relation to histological subtypes and dual pathology. Brain 127, 2406–2418. http://dx.doi.org/10.1093/brain/awh277.

Gnatkovsky, V., Librizzi, L., Trombin, F., de Curtis, M., 2008. Fast activity at seizure onset is mediated by inhibitory circuits in the entorhinal cortex in vitro. Ann. Neurol. 64, 674–686. http://dx.doi.org/10.1002/ana.21519.

Heers, M., Hedrich, T., An, D., Dubeau, F., Gotman, J., Grova, C., Kobayashi, E., 2014. Spatial correlation of hemodynamic changes related to interictal epileptic discharges with electric and magnetic source imaging. Hum. Brain Mapp. 35, 4396–4414. http://dx.doi.org/10.1002/hbm.22482.

Helias, M., Tetzlaff, T., Diesmann, M., 2013. Echoes in correlated neural systems. New J. Phys. 15.

Helias, M., Tetzlaff, T., Diesmann, M., 2014. The correlation structure of local neuronal networks intrinsically results from recurrent dynamics. PLoS Comput. Biol. 10, e1003428. http://dx.doi.org/10.1371/journal.pcbi.1003428.

Henle, C., Raab, M., Cordeiro, J.G., Doostkam, S., Schulze-Bonhage, A., Stieglitz, T., Rickert, J., 2011. First long term in vivo study on subdurally implanted micro-ECoG electrodes, manufactured with a novel laser technology. Biomed. Microdevices 13, 59–68. http://dx.doi.org/10.1007/s10544-010-9471-9.

Izhikevich, E.M., 2000. Neural excitability, spiking and bursting. Int. J. Bifurcation Chaos 10, 1171–1266. http://dx.doi.org/10.1142/S0218127400000840.

Jacobs, J., Levan, P., Chatillon, C.E., Olivier, A., Dubeau, F., Gotman, J., 2009. High frequency oscillations in intracranial EEGs mark epileptogenicity rather than lesion type. Brain 132, 1022–1037. http://dx.doi.org/10.1093/brain/awn351.

Jacobs, J., Zijlmans, M., Zelmann, R., Chatillon, C.-E., Hall, J., Olivier, A., Dubeau, F., Gotman, J., 2010. High-frequency electroencephalographic oscillations correlate with outcome of epilepsy surgery. Ann. Neurol. 67, 209–220. http://dx.doi.org/10.1002/ana.21847.

Jirsa, V.K., Stacey, W.C., Quilichini, P.P., Ivanov, A.I., Bernard, C., 2014. On the nature of seizure dynamics. Brain 137, 2210–2230. http://dx.doi.org/10.1093/brain/awu133.

Jiruska, P., de Curtis, M., Jefferys, J.G., Schevon, C.A., Schiff, S.J., Schindler, K., 2013. Synchronization and desynchronization in epilepsy: controversies and hypotheses. J. Physiol. 591, 787–797. http://dx.doi.org/10.1113/jphysiol.2012.239590.

Kendall, M.G., 1970. Rank Correlation Methods. Griffin, London.

Koti, K.M., Babu, G.J., 1996. Sign test for ranked-set sampling. Commun. Stat. Theory Methods 25, 1617–1630.

Lee, S.I., Messenheimer, J.A., Wilkinson, E.C., Brickley Jr., J.J., Johnson, R.N., 1980. Visual evoked potentials to stimulus trains: normative data and application to photosensitive seizures. Electroencephalogr. Clin. Neurophysiol. 48, 387–394.

Mangin, J.F., Frouin, V., Bloch, I., Régis, J., López-Krahe, J., 1995. From 3D magnetic resonance images to structural representations of the cortex topography using topology preserving deformations. J. Math. Imaging Vis. 5, 297–318. http://dx.doi.org/10.1007/BF01250286.

Medici, V., Rossini, L., Deleo, F., Tringali, G., Tassi, L., Cardinale, F., Bramerio, M., de Curtis, M., Garbelli, R., Spreafico, R., 2016. Different parvalbumin and GABA expression in human epileptogenic focal cortical dysplasia. Epilepsia 57, 1109–1119. http://dx.doi.org/10.1111/epi.13405.

Menezes Cordeiro, I., von Ellenrieder, N., Zazubovits, N., Dubeau, F., Gotman, J., Frauscher, B., 2015. Sleep influences the intracerebral EEG pattern of focal cortical dysplasia. Epilepsy Res. 113, 132–139. http://dx.doi.org/10.1016/j.eplepsyres.2015.03.014.

Metz, C.E., 1986. ROC methodology in radiologic imaging. Investig. Radiol. http://dx.doi.org/10.1097/00004424-198609000-00009.

Nakagawa, J.M., Donkels, C., Fauser, S., Schulze-Bonhage, A., Prinz, M., Zentner, J., Haas, C.A., 2017. Characterization of focal cortical dysplasia with balloon cells by layer-specific markers: evidence for differential vulnerability of interneurons. Epilepsia 58, 635–645. http://dx.doi.org/10.1111/epi.13690.

Ngui, A.K., Bottomley, C., Kleinschmidt, I., Sander, J.W., Newton, C.R., 2010. Estimation of the burden of active and life-time epilepsy: a meta-analytic approach. Epilepsia 51, 883–890. http://dx.doi.org/10.1111/j.1528-1167.2009.02481.x.

Nobili, L., Cardinale, F., Magliola, U., Cicolin, A., Didato, G., Bramerio, M., Fuschillo, D., Spreafico, R., Mai, R., Sartori, I., Francione, S., Lo Russo, G., Castana, L., Tassi, L., Cossu, M., 2009. Taylor's focal cortical dysplasia increases the risk of sleep-related epilepsy. Epilepsia 50, 2599–2604.

Palmini, A., Najm, I., Avanzini, G., Babb, T., Guerrini, R., Foldvary-Schaefer, N., Jackson, G., Luders, H.O., Prayson, R., Spreafico, R., Vinters, H.V., 2004. Terminology and classification of the cortical dysplasias. Neurology 62, S2–8.

Ren, L., Kucewicz, M.T., Cimbalnik, J., Matsumoto, J.Y., Brinkmann, B.H., Hu, W., Marsh, W.R., Meyer, F.B., Stead, S.M., Worrell, G.A., 2015. Gamma oscillations precede interictal epileptiform spikes in the seizure onset zone. Neurology 84, 602–608. http://dx.doi.org/10.1212/WNL.0000000000001234.

Rosenow, F., Lüders, H., 2001. Presurgical evaluation of epilepsy. Brain 124, 1683–1700.

Schuele, S., Lüders, H., 2008. Intractable epilepsy: management and therapeutic alternatives. Lancet Neurol. 7, 514–524. http://dx.doi.org/10.1016/S1474-4422(08)70108-X.

Spreafico, R., Battaglia, G., Arcelli, P., Andermann, F., Dubeau, F., Palmini, A., Olivier, A., Villemure, J.G., Tampieri, D., Avanzini, G., Avoli, M., 1998. Cortical dysplasia: an immunocytochemical study of three patients. Neurology 50, 27–36.

Staba, R.J., Frighetto, L., Behnke, E.J., Mathern, G.W., Fields, T., Bragin, A., Ogren, J., Fried, I., Wilson, C.L., Engel Jr., J., 2007. Increased fast ripple to ripple ratios correlate with reduced hippocampal volumes and neuron loss in temporal lobe epilepsy patients. Epilepsia 48, 2130–2138. http://dx.doi.org/10.1111/j.1528-1167.2007.01225.x.

Stead, M., Bower, M., Brinkmann, B.H., Lee, K., Marsh, W.R., Meyer, F.B., Litt, B., Van Gompel, J., Worrell, G.A., 2010. Microseizures and the spatiotemporal scales of human partial epilepsy. Brain 133, 2789–2797. http://dx.doi.org/10.1093/brain/awq190.

Tadel, F., Baillet, S., Mosher, J.C., Pantazis, D., Leahy, R.M., 2011. Brainstorm: a user-friendly application for MEG/EEG analysis. Comput. Intell. Neurosci. 2011. http://dx.doi.org/10.1155/2011/879716.

Tassi, L., Garbelli, R., Colombo, N., Bramerio, M., Russo, G. Lo, Mai, R., Deleo, F., Francione, S., Nobili, L., Spreafico, R., 2012. Electroclinical, MRI and surgical outcomes in 100 epileptic patients with type II FCD. Epileptic Disord. 14, 257–266. http://dx.doi.org/10.1684/epd.2012.0525.

van Vreeswijk, C., Sompolinsky, H., 1996. Chaos in neuronal networks with balanced excitatory and inhibitory activity. Science 80 (274), 1724–1726.

von Ellenrieder, N., Pellegrino, G., Hedrich, T., Gotman, J., Lina, J.M., Grova, C., Kobayashi, E., 2016. Detection and Magnetic Source Imaging of Fast Oscillations (40–160 Hz) Recorded with Magnetoencephalography in Focal Epilepsy Patients. Brain Topogr. 29, 218–231. http://dx.doi.org/10.1007/s10548-016-0471-9.

Wagner, J., Weber, B., Urbach, H., Elger, C.E., Huppertz, H.J., 2011. Morphometric MRI analysis improves detection of focal cortical dysplasia type II. Brain 134, 2844–2854. http://dx.doi.org/10.1093/brain/awr204.

Wendling, F., Bartolomei, F., Bellanger, J.J., Chauvel, P., 2002. Epileptic fast activity can be explained by a model of impaired GABAergic dendritic inhibition. Eur. J. Neurosci. 15, 1499–1508.

Worrell, G.A., Parish, L., Cranstoun, S.D., Jonas, R., Baltuch, G., Litt, B., 2004. High-frequency oscillations and seizure generation in neocortical epilepsy. Brain 127, 1496–1506. http://dx.doi.org/10.1093/brain/awh149.

Zarrelli, M.M., Beghi, E., Rocca, W.A., Hauser, W.A., 1999. Incidence of epileptic syndromes in Rochester, Minnesota: 1980–1984. Epilepsia 40, 1708–1714.

Zijlmans, M., Jiruska, P., Zelmann, R., Leijten, F.S.S., Jefferys, J.G.R., Gotman, J., 2012. High-frequency oscillations as a new biomarker in epilepsy. Ann. Neurol. 71, 169–178. http://dx.doi.org/10.1002/ana.22548.

Zijlmans, M., Worrell, G.A., Dümpelmann, M., Stieglitz, T., Barborica, A., Heers, M., Ikeda, A., Usui, N., Le Van Quyen, M., 2017. How to record high-frequency oscillations in epilepsy: a practical guideline. Epilepsia 1–11. http://dx.doi.org/10.1111/epi.13814.